Medical Engineering and Physics 66 (2019) 96–101

Contents lists available at ScienceDirect

Medical Engineering and Physics

journal homepage: www.elsevier.com/locate/medengphy

Technical note

A method to estimate inertial properties and force plate inertial components for instrumented platforms

Brad W.R. Roberts[a], Jeremy C. Hall[b], Andrew D. Williams[b], Hossein Rouhani[a,b,c], Albert H. Vette[a,b,c,*]

[a] Department of Mechanical Engineering, University of Alberta, 10-203 Donadeo Innovation Centre for Engineering, 9211 116 Street NW, Edmonton, Alberta T6G 1H9, Canada
[b] Department of Biomedical Engineering, University of Alberta, 1098 Research Transition Facility, Edmonton, Alberta T6G 2V2, Canada
[c] Glenrose Rehabilitation Hospital, Alberta Health Services, 10230 111 Avenue NW, Edmonton, Alberta T5G 0B7, Canada

ARTICLE INFO

Article history:
Received 28 June 2018
Accepted 10 February 2019

Keywords:
Dynamic posturography
Force plate
Instrumented platform
Inverse dynamics
Kinematics
Postural control

ABSTRACT

Kinetic data acquired from force plates embedded in moving platforms naturally contain artifacts due to platform acceleration, called force plate inertial components. While they can be estimated and removed from the measured signals, the system's inertial properties need to be known. Our objective was to: (1) develop a method for estimating the inertial properties and force plate inertial components for any instrumented platform; (2) estimate the inertial properties specifically for the Computer-Assisted Rehabilitation Environment (CAREN); and (3) validate the estimates with new experimental data. Unloaded ramp-and-hold perturbations (for estimation) and unloaded random perturbations (for validation) were executed to obtain the force, moment, and motion of the CAREN platform. Inertial properties were estimated by minimizing the error between the measured and computed inertial forces and moments. Obtained estimates were validated by calculating the coefficient of determination (R^2) between the measured and computed forces or moments when keeping the inertial properties fixed. The estimates of the CAREN's inertial properties exhibited low variability across trials, and R^2 for the validation trials was 0.90 ± 0.08 (mean ± standard deviation). The developed method can be used for removing inertial components from force plate signals, yielding reliable estimates of ground reactions in dynamic biomechanical research and clinical assessments.

1. Introduction

The primary objective of human postural control is to maintain the body in a stable, upright position. While this task appears to be simple, it is accomplished by a complex process that takes advantage of previous experience (*feed-forward control*) [1,2] and seamless integration of sensory information (*feedback control*) [2–4]. Although the principles of postural control are generally understood, current efforts aim to shed light on the specific neurophysiological mechanisms the central nervous system applies to accomplish this task. Such mechanistic understanding is critical for clinicians seeking to identify balance deficits and optimize treatment in patient populations.

Postural perturbations displacing the body's center of mass (CoM) are commonly used to study the control of posture [3,5]. One of the most common forms of perturbations used in fundamental investigations is to disturb the support surface on which an individual is standing. Movement of the support surface, either through translation or rotation, displaces the base of support relative to the CoM, thus necessitating a neuromuscular reaction to reposition the CoM over the displaced base of support [3]. This is accomplished by means of timely, stabilizing moments that are globally reflected in the body's center of pressure fluctuation. Using an *instrumented platform* – defined as a moving platform embedding a single or multiple force plates – the trajectory of the center of pressure may be recorded and used to characterize postural stability and control, referred to as dynamic posturography. Depending on the application, different perturbation profiles are available, including ramp-and-hold, impulse, sinusoidal, or randomized profiles [6].

The need for an instrumented platform implies that studies involving dynamic posturography require complex and costly equipment. While multiple options are available [7–13], many of these

* Corresponding author at: Neuromuscular Control & Biomechanics Laboratory, Department of Mechanical Engineering, University of Alberta, 10-203 Donadeo Innovation Centre for Engineering, 9211 116 Street NW, Edmonton, Alberta, T6G 1H9, Canada.
E-mail address: albert.vette@ualberta.ca (A.H. Vette).

https://doi.org/10.1016/j.medengphy.2019.02.012
1350-4533/

systems are restricted to translations along, or rotations about, a finite set of principle axes [7]. However, one system in particular, the extended Computer-Assisted Rehabilitation Environment (CAREN; Motek Medical, Amsterdam, The Netherlands), employs a hydraulically actuated instrumented platform capable of delivering 6-degree of freedom perturbations. In addition, it includes: a 180-degree projection screen; a surround-sound audio system; a 12-camera motion capture system; and a dual-belt treadmill mounted above two force plates. With all of these features available, the CAREN seems optimal for all types of fundamental and rehabilitation research, including dynamic posturography. Unfortunately, such use is not always realistic as having the force plates embedded within the platform renders the data unreliable: in moving the force plates, the acquired forces and moments will contain components due to accelerating the total mass resting on the force plates' transducers, termed *force plate inertial components* (FPIC) [14]. Therefore, the CAREN's platform-embedded force plates can only be used to reliably measure kinetic data when the platform is stationary – as there is currently no accepted method to remove FPIC from CAREN force plate data [15,16]. This is, however, a problem not only for the force plates of the CAREN, but of any moving platform.

To solve the FPIC issue, Preuss and Fung [14] introduced a method to isolate and reduce the effect of these components using motion capture and inverse dynamics. In tracking the moving base, they used the obtained position data along with the inertial properties of the platform (mass, moment of inertia, and position of platform's CoM relative to the force plate's transducers) to estimate the FPIC. A comparison between the predicted and acquired force plate signals validated the use of motion capture and inverse dynamics to reliably reduce FPIC from force plate data collected under dynamic conditions. Other potential methods to remove FPIC use accelerometers instead of motion capture [17,18]. Given that the CAREN is already equipped with a motion capture system, the approach outlined by Preuss and Fung [14] offers the most suitable option to estimate and remove FPIC. The fundamental drawback of this method is, however, that it requires knowledge of the inertial properties of the platform. In addition, the assumption of symmetry suggests that the CoM lies directly above the average force plate transducer location, which further limits the method's application.

Oftentimes, for systems such as the CAREN, the inertial properties may be unknown, or vary between models. In addition, it is possible that the FPIC are affected by secondary components integrated into a given system (e.g., the treadmill in the CAREN). With that in mind, it is essential that a method be derived allowing users of the CAREN, or similar instrumented platforms, to estimate the inertial properties specific to their system, with the ultimate goal of removing the FPIC from the force plate measurements. The purpose of this study was therefore to: (1) outline a simple method for estimating the inertial properties and force plate inertial components for any instrumented platform; (2) estimate those properties specifically for the CAREN extended system; and (3) validate the obtained estimates via new experimental data.

2. Methods

2.1. Force plate signals

Force plate signals obtained during studies of dynamic posturography are a combination of ground reactions (applied to the force plate by the perturbed human) and inertial components (created by both motion and gravity of the platform). Therefore, the measured force plate force, $\vec{F}$, and moment, $\vec{M}$, expressed in the platform coordinate system (PCS) provided in Fig. 1, are:

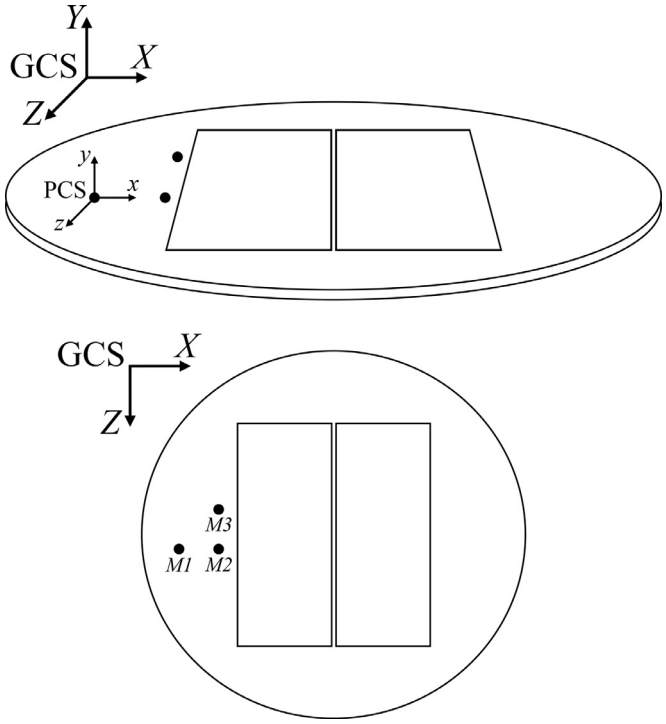

Fig. 1. The orientations of the CAREN platform in its starting orientation relative to the global coordinate system (GCS); and of the platform coordinate system (PCS) relative to the CAREN platform. Three markers (*M1*, *M2*, and *M3*) were placed on the platform to define PCS, with *M1* and *M2* forming a line parallel to the *x* axis.

$$\begin{aligned}\vec{F} &= \vec{F}_{GR} + \vec{F}_I \\ \vec{M} &= \vec{M}_{GR} + \vec{M}_I\end{aligned} \tag{1}$$

where $\vec{F}_{GR}$ and $\vec{M}_{GR}$ are the ground reaction force and moment, respectively; and $\vec{F}_I$ and $\vec{M}_I$ are the inertial force and moment, respectively. Note that the force plate signals are assumed to be zeroed when the platform is in its starting orientation. The components of the inertial force are:

$$\begin{bmatrix} F_{I_x} \\ F_{I_y} \\ F_{I_z} \end{bmatrix} = m \begin{bmatrix} a_x \\ a_y \\ a_z \end{bmatrix} + R_{xyz}^{T} \begin{bmatrix} 0 \\ mg \\ 0 \end{bmatrix} - \begin{bmatrix} 0 \\ mg \\ 0 \end{bmatrix} \tag{2}$$

where m is the mass resting on the force plate transducers; a_x, a_y, and a_z are the components of the linear acceleration of the platform's CoM, $\vec{a}$, expressed in PCS; R_{xyz} is the rotation matrix capturing the orientation of PCS relative to the global coordinate system (GCS) provided in Fig. 1; and g is the acceleration due to gravity. The components of the inertial moment are:

$$\begin{aligned} M_{I_x} &= I_x\alpha_x + d_yF_{I_z} - d_zF_{I_y} \\ M_{I_y} &= I_y\alpha_y - d_xF_{I_z} + d_zF_{I_x} \\ M_{I_z} &= I_z\alpha_z + d_xF_{I_y} - d_yF_{I_x} \end{aligned} \tag{3}$$

where I_x, I_y, and I_z are the principal components of the moment of inertia, $\vec{I}$, of the mass resting on the force plate transducers; α_x, α_y, and α_z are the components of the angular acceleration, $\vec{\alpha}$, of the platform; and d_x, d_y, and d_z are the components of the position, $\vec{d}$, of the CoM relative to the average force plate transducer location. Note that $\vec{I}$, $\vec{\alpha}$, and $\vec{d}$ are expressed in PCS. Detailed derivations of the components of $\vec{F}_I$ and $\vec{M}_I$ and of the PCS are provided in Supplements S1 and S2, respectively.

2.2. Experimental procedure and data acquisition

To estimate the inertial properties m, $\vec{I}$, and $\vec{d}$ of the CAREN (see Section 2.3.2), two unloaded estimation trials (i.e., without a human user) were executed. Both estimation trials had ramp-and-hold perturbation profiles. The first estimation trial consisted of translations in the positive direction of each of the *x, y*, and *z* axes (Fig. 1) followed by a return to the starting position. Translations from the starting position to maximum displacement, and vice versa, were 12 cm in 0.5 s, with a 3 s hold of maximum displacement [19–22]. Five translations were performed for each axis, for a total of fifteen translations. The second estimation trial consisted of positive rotations about each of the *x, y*, and *z* axes (Fig. 1) followed by a return to the starting orientation. Rotations from the starting orientation to maximum angular displacement, and vice versa, were 7.5° in 0.5 s, with a 3 s hold of maximum angular displacement [23–25]. Five rotations were performed for each axis, for a total of fifteen rotations.

To validate the estimated inertial properties (see Section 2.3.3), two unloaded validation trials were executed. Both validation trials had random perturbation profiles. The first validation trial consisted of random translations [16,26–28] along each of the *x, y*, and *z* axes (Fig. 1). Five 10 s translations were performed for each axis, for a total of fifteen translations. The second validation trial consisted of random rotations [16,26–28] about each of the *x, y*, and *z* axes (Fig. 1). Five 10 s rotations were performed for each axis, for a total of fifteen rotations. Different perturbation profiles were used across the three translation (rotation) axes, but the same perturbation profile was used for all five translations (rotations) of a given axis.

Force and moment data were recorded at a sampling frequency of 1000 Hz [15,16] using two force plates (Bertec Corporation, Columbus, USA) embedded within the treadmill of the CAREN. Raw force plate data were down-sampled to 100 Hz and filtered using a fourth-order, zero phase-shift, low-pass Butterworth filter with a cut-off frequency of 5 Hz [15,16]. Platform motion data were recorded at 100 Hz [15,16] using a 12-camera motion capture system (MX T20S, Vicon Inc., Oxford, UK). Three markers (*M1, M2*, and *M3*) were placed on the platform, with *M1* and *M2* defining a line parallel to the *x* axis (Fig. 1). Raw marker data were filtered using a second-order, zero phase-shift, low-pass Butterworth filter with a cut-off frequency of 4 Hz [15,16]. Note that raw force plate and marker data were expressed in PCS and GCS, respectively.

2.3. Experimental data analysis

2.3.1. Platform kinematics

The position of the platform was calculated as the average of *M1, M2*, and *M3*. The linear acceleration of the platform, expressed in GCS, was then calculated from the position of the platform using finite difference equations [29]. Finally, the linear acceleration of the platform, $\vec{a}$, expressed in PCS, was calculated using its representation in GCS and R_{xyz}. The platform angles θ_x, θ_y, and θ_z were calculated from R_{xyz} using the Cardan *xyz* sequence [30]. The angular acceleration of the platform was then calculated from the angular displacement of the platform using finite difference equations [29]. Equations for $\vec{a}$, R_{xyz}, and the Cardan *xyz* sequence are provided in Supplement S3.

2.3.2. Estimation of inertial properties

Referring to Eq. (1), since the platform was unloaded (i.e., $\vec{F}_{GR} = \vec{M}_{GR} = 0$) for both the estimation and validation trials, $\vec{F} = \vec{F}_I$ and $\vec{M} = \vec{M}_I$. The inertial properties were therefore estimated by finding the values that minimized the sum of squared errors (SSE) between the force and moment recorded in the estimation trials and the computed, *reduced* inertial force and moment, respectively. Specifically, m and $\vec{d}$ were estimated from the translation, and $\vec{I}$ from the rotation trial data. The *reduced* inertial force and moment equations were derived from Eqs. (2) and (3) by setting variables to zero that were theoretically zero (e.g., $a_y = 0$ for *x* translations) and replacing $\vec{F}_I$ components with corresponding $\vec{F}$ components in $\vec{M}_I$. Detailed derivations of the *reduced* inertial force and moment in unloaded platform translations and rotations are provided in Supplements S4 and S5, respectively.

For *x* translations, the SSE expressions that were minimized are:

$$\begin{aligned} SSE_{F_x}(m) &= \sum_{i=1}^{N} [F_x(i) - \boldsymbol{m}a_x(i)]^2 \\ SSE_{M_y}(d_z) &= \sum_{i=1}^{N} [M_y(i) - \boldsymbol{d_z}F_x(i)]^2 \\ SSE_{M_z}(d_y) &= \sum_{i=1}^{N} [M_z(i) + \boldsymbol{d_y}F_x(i)]^2 \end{aligned} \quad (4)$$

where N is the total number of samples per translation (excluding hold time). Estimates of m, d_y, and d_z (bold in Eq. (4)) were obtained for each *x* translation, for a total of five estimates of each. The SSE expressions for *y* and *z* translations are similar. Note that m, d_x, and d_z estimates were obtained from *y* translations, and m, d_x, and d_y estimates were obtained from *z* translations. Overall m and $\vec{d}$ values (mean ± standard deviation) were calculated from the estimates from all translations.

For *x* rotations, the SSE expression that was minimized is:

$$SSE_{M_x}(I_x) = \sum_{i=1}^{N} [M_x(i) - (\boldsymbol{I_x}\alpha_x(i) + d_yF_z(i) - d_zF_y(i))]^2 \quad (5)$$

where N is as before, but for rotations, and d_y and d_z are mean estimates identified earlier. An estimate of I_x (bold in Eq. (5)) was obtained for each *x* rotation, for a total of five estimates. The SSE expressions for *y* and *z* rotations are similar. Note that I_y and I_z estimates were obtained from *y* and *z* rotations, respectively. Overall $\vec{I}$ values (mean ± standard deviation) were calculated from the estimates from all rotations.

SSE expressions were minimized using the function *fminsearch* in MATLAB (version R2017a, MathWorks, Natick, United States). A complete set of SSE expressions is provided in Supplement S6.

2.3.3. Validation of estimated inertial properties

The mean estimates of the inertial properties and the equations for the inertial components were validated by calculating, for all estimation and validation data, the coefficient of determination (R^2) between the measured and computed force or moment. Overall R^2 values (mean ± standard deviation) were reported for estimation and validation trials separately.

3. Results

3.1. Inertial properties of the CAREN extended system

Fig. 2 depicts representative time series of the linear displacement (A) and acceleration (C) of the unloaded CAREN platform, along with the measured force F_x (B) and moment M_z (D), for a ramp-and-hold *x* translation in an estimation trial. The 0.5 s intervals of the translation used to estimate m and d_y are marked with bold lines. It can be clearly seen that the measured force F_x and moment M_z are affected by the motion of the platform.

In Table 1, the estimated inertial properties of the CAREN are presented (mean ± standard deviation). Listed are the values calcu-

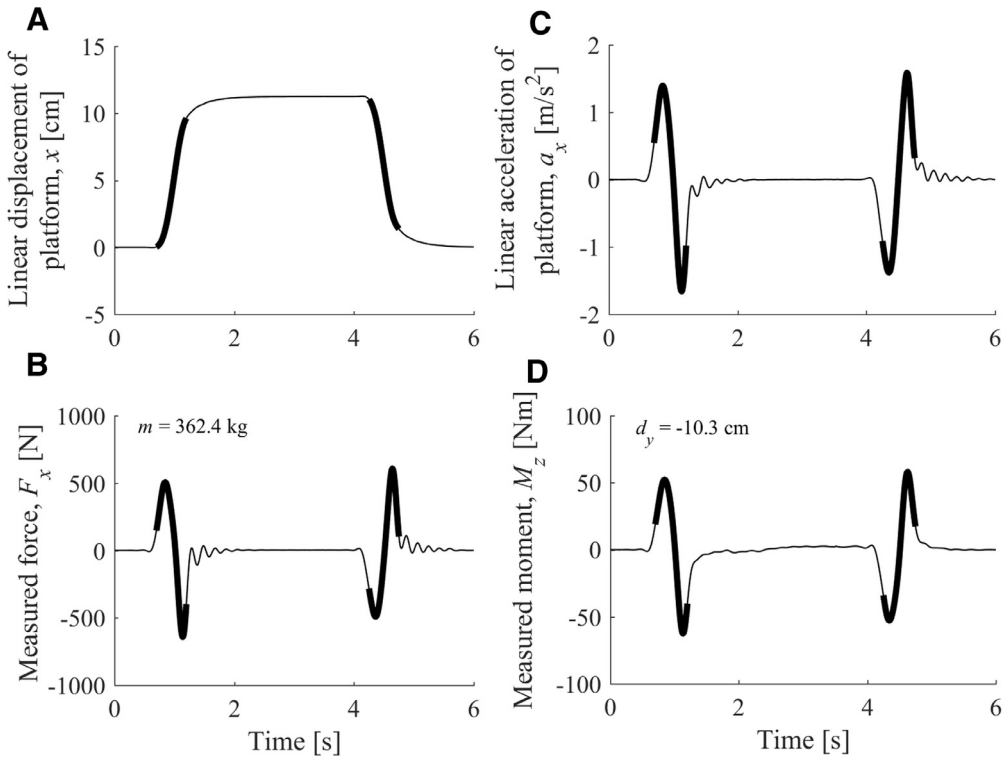

Fig. 2. Representative platform motion and corresponding force plate time series for a ramp-and-hold x translation in an estimation trial. A and C: linear displacement and acceleration of the platform; B and D: corresponding measured force F_x and moment M_z. Bold lines mark the 0.5 s intervals of the translation used to estimate the mass resting on the force plate transducers, m, and the y component of the position of the center of mass relative to the average force plate transducer location, d_y. Estimates of m and d_y obtained from the translation are shown.

Table 1
Estimated inertial properties of the CAREN extended system. Listed are the values calculated for each axis (from five estimates for translations and five estimates for rotations) and across all movements. All values are presented as mean ± standard deviation.

Axis and direction	Inertial property						
	m [kg]	d_x [cm]	d_y [cm]	d_z [cm]	I_x [kg m^2]	I_y [kg m^2]	I_z [kg m^2]
x	362.3 ± 0.1	–	−10.5 ± 0.1	−8.3 ± 0.1	139.5 ± 2.5	–	–
y	356.3 ± 1.0	−0.2 ± 0.0	–	−13.3 ± 0.2	–	165.1 ± 1.2	–
z	351.0 ± 0.6	0.3 ± 0.1	−6.9 ± 0.3	–	–	–	46.3 ± 0.2
Overall	**356.5 ± 4.8**	**0.0 ± 0.3**	**−8.7 ± 2.0**	**−10.8 ± 2.6**	**139.5 ± 2.5**	**165.1 ± 1.2**	**46.3 ± 0.2**

lated for each axis (from five estimates for translations and five estimates for rotations) and across all movements. The overall value for d_x (0.0 ± 0.3 cm) indicates that the CAREN platform is symmetrical with respect to its yz plane.

3.2. Validation of computed inertial force and moment

Fig. 3A and B depict representative time series of the linear displacement of the CAREN platform and the measured force F_x (black line), respectively, for a random x translation in a validation trial. Fig. 3C and D depicts representative time series of the platform angle θ_x and the measured moment M_x (black line), respectively, for a random x rotation in a validation trial. In Fig. 3B and D, the measured force F_x and moment M_x are compared to the computed force F_{l_x} and moment M_{l_x} (gray lines), respectively. A visual inspection and respective R^2 values for the translation (R^2 = 0.94) and rotation (R^2 = 0.96) suggest the ability of Eq. (2) and (3) to estimate the inertial force and moment in CAREN force plate signals.

In Table 2, overall R^2 values (mean ± standard deviation) for estimation and validation trials are presented. Also presented are values calculated from the five R^2 values from each translation or rotation, for each component of the measured force and moment. The overall R^2 value for the validation trials (0.90 ± 0.08) confirms that the mean estimates of the inertial properties, together with Eq. (2) and (3), can predict the inertial force and moment in CAREN force plate signals.

4. Discussion

The objectives of the present study were to develop a method for estimating the inertial properties and FPIC for any instrumented platform, and to estimate and validate the inertial properties specifically for the CAREN. Low variability of the estimated inertial properties for the CAREN (see Table 1) and excellent agreement between the measured and computed force or moment (see Fig. 3 and Table 2) confirm the adequacy of the developed method to meet our objectives. It can be used for removing inertial components from force plate signals, yielding reliable estimates of ground reactions in biomechanical research and clinical assessments. In what follows, we recommend a simplified experimental procedure and assumptions for $\vec{d}$ for symmetrical platforms, dis-

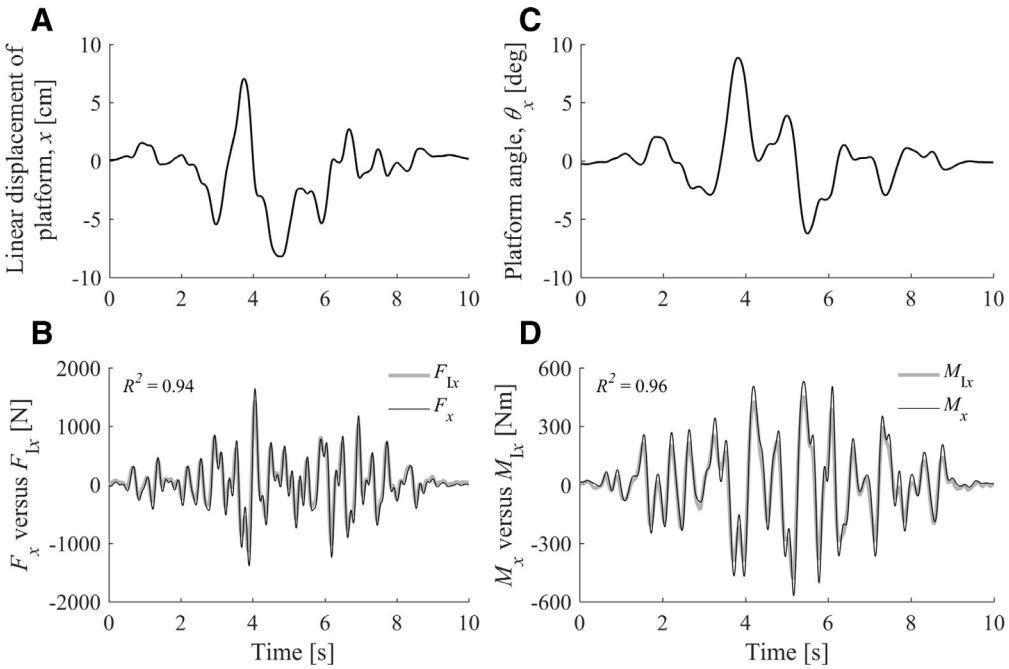

Fig. 3. Representative platform motion and corresponding force plate time series for a random x translation (A and B) and rotation (C and D) in the validation trials. A and B: linear displacement of the platform, x, and comparison between the x component of the corresponding measured force (black) and the computed inertial force (gray). The coefficient of determination, R^2, between the forces was $R^2 = 0.94$. C and D: platform angle about the x axis, θ_x, and comparison between the x component of the corresponding measured moment (black) and the computed inertial moment (gray). The coefficient of determination between the moments was $R^2 = 0.96$.

Table 2
Coefficient of determination (R^2) values between the measured force and moment and the computed inertial force and moment, respectively. Shown are overall R^2 values for estimation (ramp-and-hold) and validation (random) trials. Also shown are values calculated from the five R^2 values from each translation or rotation, for each component of the measured force and moment. All values are presented as mean ± standard deviation.

		Axis	Coefficient of determination (R^2)					
			F_x	F_y	F_z	M_x	M_y	M_z
Ramp-and-hold	***Trans.***	***x***	0.98 ± 0.00	–	–	–	0.94 ± 0.02	0.94 ± 0.01
		y	–	0.98 ± 0.00	–	0.90 ± 0.01	–	–
		z	–	–	0.98 ± 0.00	0.89 ± 0.03	–	–
	Rot.	***x***	–	–	–	0.98 ± 0.00	–	–
		y	–	–	–	–	0.99 ± 0.00	–
		z	–	–	–	–	–	0.99 ± 0.00
Random	***Trans.***	***x***	0.94 ± 0.00	–	–	–	0.87 ± 0.01	0.88 ± 0.01
		y	–	0.96 ± 0.00	–	0.85 ± 0.01	–	–
		z	–	–	0.94 ± 0.00	0.70 ± 0.03	–	–
	Rot.	***x***	–	–	–	0.96 ± 0.00	–	–
		y	–	–	–	–	0.96 ± 0.00	–
		z	–	–	–	–	–	0.96 ± 0.00

Overall ramp-and-hold: 0.96 ± 0.04; overall random: 0.90 ± 0.08.

cuss alternative SSE expressions, and elaborate on how overall R^2 values were calculated.

4.1. Simplified procedure and considerations for symmetrical platforms

Based on an inspection of the variability of the CAREN inertial property values presented in Table 1, a *simplified* experimental procedure is recommended. Specifically, in the estimation trial used to estimate m and $\vec{d}$ (translations), we recommend that only one translation be performed for each axis, for a total of three translations. Additionally, in the estimation trial used to estimate $\vec{I}$ (rotations), we recommend that only one rotation be performed for each axis, for a total of three rotations.

For platforms that are known to be symmetrical with respect to only one of their xy and yz planes (i.e., *partial* symmetry), we recommend d_z be assumed zero (for xy plane symmetry) or d_x be assumed zero (for yz plane symmetry) and not calculated from acquired force, moment, and platform motion data. Since the CAREN extended system is symmetrical with respect to its yz plane, we recommend that, for this system, d_x be assumed zero. For platforms that are known to be symmetrical with respect to both their xy and yz planes (i.e., *full* symmetry), we recommend both d_x and d_z be assumed zero. Note that the method to estimate and remove FPIC introduced by Preuss and Fung [14] assumes *full* symmetry and should therefore not be applied if the platform does not possess *full* symmetry. However, if the platform is known to possess *full* symmetry, their method to estimate and remove FPIC is equivalent to the one developed here. Nevertheless, it assumes knowledge of the inertial properties of the platform.

4.2. Alternative to reduced method for estimating inertial properties

The *reduced* inertial force and moment used in the SSE expressions (see Methods section) were chosen in this work because they provide a *simple* method for estimating the inertial properties of a

platform. Alternative SSE expressions may be developed that find inertial property values that minimize the SSE between the measured force and moment and the inertial force and moment computed using Eqs. (2) and (3), respectively. However, these SSE expressions would be coupled and therefore require a simultaneous approach in solving them. Moreover, we expect that this alternative, more involved approach would yield similar inertial property estimates to those obtained here, since: (1) the simplifying assumptions made in deriving the *reduced* inertial force and moment (see Supplements S4 and S5) are justified; and (2) the overall R^2 value for the validation trials (0.90 ± 0.08) indicates that the mean estimates of the inertial properties are acceptable.

4.3. Values used in calculating overall R^2 values

Overall R^2 values for estimation and validation trials were calculated using only R^2 values from select components of the measured force and moment depending on the axis (i.e., *x*, *y*, or *z*) and perturbation type (i.e., translation or rotation) (see Table 2). For a particular axis and type of perturbation, R^2 values from force and moment components were excluded (and not reported in Table 2) if the force and moment components: (1) were theoretically zero (e.g., F_y and M_x for *x* translations); (2) negligibly small due to d_x being negligibly small (e.g., M_z for *y* translations); or (3) otherwise negligibly small (e.g., all components of $\vec{F}$, M_y, and M_z for *x* rotations).

Acknowledgments

We would like to thank Darrell Goertzen for his contributions to CAREN programming and experimental data acquisition.

Competing interests

None declared.

Funding

This study was partially funded through a Discovery Grant from the Natural Sciences and Engineering Research Council of Canada (RGPIN-2014-04666).

Ethical approval

Not required.

Supplementary material

Supplementary material associated with this article can be found, in the online version, at doi:10.1016/j.medengphy.2019.02.012.

References

[1] Massion J. Movement, posture and equilibrium: interaction and coordination. Prog Neurobiol 1992;38:35–56.
[2] Tjernström F, Fransson PA, Patel M, Magnusson M. Postural control and adaptation are influenced by preceding postural challenges. Exp Brain Res 2010;202:613–21.
[3] Chen C-L, Lou S-Z, Wu H-W, Wu S-K, Yeung K-T, Su F-C. Effects of the type and direction of support surface perturbation on postural responses. J Neuroeng Rehabil 2014;11:50.
[4] Mancini M, Horak FB. The relevance of clinical balance assessment tools to differentiate balance deficits. Eur J Phys Rehabil Med 2010;46:239–48.
[5] Horak FB, Henry SM, Shumway-Cook a. Postural perturbations: new insights for treatment of balance disorders. Phys Ther 1997;77:517–33.
[6] Vette AH, Sanin E, Bulsen A, Morris A, Masani K, Popovic MR. A portable and automated postural perturbation system for balance assessment, training, and neuromuscular system identification. J Med Device 2008;2:041007.
[7] Chen C-L, Lee J-Y, Horng R-F, Lou S-Z, Su F-C. Development of a three-degrees-of-freedom moveable platform for providing postural perturbations. Proc Inst Mech Eng Part H J Eng Med 2009;223:87–97.
[8] Bassi Luciani L, Genovese V, Monaco V, Odetti L, Cattin E, Micera S. Design and Evaluation of a new mechatronic platform for assessment and prevention of fall risks. J Neuroeng Rehabil 2012;9:51.
[9] Motek Medical Gait real-time analysis interactive lab, https://www.motekforcelink.com/product/grail/; 2018 Accessed 26 June 2018.
[10] Motek Medical Dynamic stability and balance learning environment, https://www.motekforcelink.com/product/dynstable/; 2018 Accessed 26 June 2018.
[11] Peterka RJ, Goodworth AD, Mellodge P, Peterka RJ, Volpe D, Giantin MG, et al. Sensorimotor integration in human postural control. J Neurophysiol 2002;88:1097–118.
[12] Logan D, Kiemel T, Jeka JJ. Asymmetric sensory reweighting in human upright stance. PLoS One 2014;9:1–10.
[13] Fung J, Johnstone E. Lost in space. Multi-axial and multi-dimensional surface perturbations delivered by a novel motion base device [abstract]. Soc Neurosci 1998;24:1158.
[14] Preuss R, Fung J. A simple method to estimate force plate inertial components in a moving surface. J Biomech 2004;37:1177–80.
[15] Sinitski EH, Lemaire ED, Baddour N. Characteristics of a dual force plate system embedded in a six degree of freedom motion platform. In: Proceedings of the IEEE International Symposium on Medical Measurements and Applications MeMeA 2013; 2013. p. 241–5.
[16] Sinitski EH, Lemaire ED, Baddour N. Evaluation of motion platform embedded with force plate-instrumented treadmill. J Rehabil Res Dev 2015;52:221–233.
[17] Pagnacco G, Silva A, Oggero E, Berme N. Inertially compensated force plate: a means for quantifying subject's ground reaction forces in non-inertial conditions. Biomed Sci Instrum 2000;36:397–402.
[18] Hnat SK, van Basten BJH, van den Bogert AJ. Compensation for inertial and gravity effects in a moving force platform. J Biomech 2018;75:96–101.
[19] Welch TDJ, Ting LH. Mechanisms of motor adaptation in reactive balance control. PLoS One 2014;9:e96440.
[20] Chvatal SA, Ting LH. Common muscle synergies for balance and walking. Front Comput Neurosci 2013;7:1–14.
[21] Torres-Oviedo G. Muscle synergies characterizing human postural responses. J Neurophysiol 2007;98:2144–56.
[22] Torres-Oviedo G, Ting LH. Subject-specific muscle synergies in human balance control are consistent across different biomechanical contexts. J Neurophysiol 2010;103:3084–98.
[23] Carpenter MG, Allum JHJ, Honegger F. Directional sensitivity of stretch reflexes and balance corrections for normal subjects in the roll and pitch planes. Exp Brain Res 1999;129:93–113.
[24] Oude Nijhuis LB, Allum JHJ, Borm GF, Honegger F, Overeem S, Bloem BR. Directional sensitivity of "first trial" reactions in human balance control. J Neurophysiol 2009;101:2802–14.
[25] Oude Nijhuis LB, Allum JHJ, Nanhoe-Mahabier W, Bloem BR. Influence of perturbation velocity on balance control in Parkinson's disease. PLoS One 2014;9:1–7.
[26] Van Der Kooij H, Van Asseldonk E, Van Der Helm FCT. Comparison of different methods to identify and quantify balance control. J Neurosci Methods 2005;145:175–203.
[27] Engelhart D, Boonstra TA, Aarts RGKM, Schouten AC, van der Kooij H. Comparison of closed-loop system identification techniques to quantify multi-joint human balance control. Annu Rev Control 2015;41:58–70.
[28] Kiemel T, Zhang Y, Jeka JJ. Identification of neural feedback for upright stance in humans: stabilization rather than sway minimization. J Neurosci 2011;31:15144–53.
[29] O'Connor CM, Thorpe SK, O'Malley MJ, Vaughan CL. Automatic detection of gait events using kinematic data. Gait Posture 2007;25:469–474.
[30] Craig JJ. 3rd Ed. Introduction to robotics: Mechanics and control, 1. Prentice Hall; 2004. p. 408.